Military Technical College
Kobry Elkobbah,
Cairo, Egypt

8th International Conference
on Aerospace Sciences &
Aviation Technology

BALANCED EARTH SATELLITE ORBITS

S.M. Elshaboury *; M. E. Awad ** and A. M. Ahmed *

Abstract

The present work aims at constructing an atlas of balanced earth satellite orbits with respect to the secular and long periodic effects of the luni-solar attractions plus the earth oblateness with the harmonics of the geopotential retained up to the 4th zonal harmonic . The variations of the elements are averaged over the fast and medium angles ,thus retaining only the secular and long periodic terms. The models obtained cover all the values of the semi major axis up to 7earth radii with the necessary avoidance of the radiation belts . The atlas obtained is useful for different purposes, with those having the semi major axis between 4 to 7earth radii particularly important for communication and television relay satellites.

Keywords

Artificial Satellites , Luni-solar attraction , earth oblateness , averaging , balanced orbits.

Nomenclature

$b=h-h_d$: difference of the nodes
Ci , $S i$: $\cos i$ and $\sin i$
i, i_d : inclinations of the sat. and the disturbing body orbits respectively.
k: constant for the 3rd body
u_d : argument of latitude of the 3rd body

*Ain Shams univ., facult. of science , Math. Dept
**Cairo univ. ,facult.of science ,Astron.and met.Dept.

1 Introduction

With the advance of the space age, it became clear that most space applications require fixing, as strictly as possible, the areas covered by the satellite or the constellation of satellites. In turn, fixing the coverage regions requires fixed nodes and fixed apsidal lines. This in turn leads to the search for orbits satisfying these requirements .

These orbits fall into two categories :"Balanced Orbits" (Kudielka [1]) and "Frozen Orbits" (Coffey et al.[2] ; and Lara et al [3]).

Clearly, the design of such orbits includes the effects of the perturbing influences that affect the motion of the satellite . As the present work is interested in H.E.O, the effects of earth oblateness and luni-solar attractions are taken into concern. These have been extensively treated in the literature (e.g Brouwer [4] ; Kozai [5] ; Kozai [6]; Musen [7] ; Cook [8] ; Lane [9] ; and Delhaise and Morbidelli [10]).

For low earth orbits, if the satellite altitude is stabilized, or at least a mean projected area could be estimated, the perturbative effects of atmospheric drag are to be included. Unfortunately, the literature is still void of even a mention of this topic of balanced low earth orbits. The reason may be the present increased interest in space communications and broadcasting which still make use of the geostationary orbits that lie beyond the effects of atmospheric drag, though they still suffer the effects of drift solar radiation pressure.

This paper is the 2nd of two papers aiming at constructing an atlas of balanced earth satellite orbits. In a previous paper (Elshabouri et al [11]), we gave a complete model for the averaged effects (over the mean anomaly) of earth oblateness and luni-solar attractions .(no conditions for the value of the semi major axis were requested).

In order to get an atlas of balanced earth satellite orbits, we have to make some simplifications on the complete model we reached in the previous paper. These simplifications are made by averaging over the intermediate angles to retain only the secular and long periodic terms. Hence we start by investigating the rates of the involved angles.

2 Choice of the models

2 .1 Model A

We will call the complete model reached in the previous paper "Model A". In this model, we gave a complete analysis for the averaged effects (over the mean anomaly) of:

1) The earth oblateness with potential up to j_4 .

2) The luni-solar attractions .

The solution is of the form:

$$\begin{aligned} \dot{e} &= \dot{e}_{ob} + \dot{e}_{ls} \\ \dot{i} &= \dot{i}_{ob} + \dot{i}_{ls} \\ \dot{h} &= \dot{h}_{ob} + \dot{h}_{ls} \\ \dot{g} &= \dot{g}_{ob} + \dot{g}_{ls} \end{aligned} \tag{1}$$

where :

$$\begin{aligned} \dot{e}_{ob} = {} & \frac{3\mu j_3 R^3}{2na^6}(1-e^2)^{-2}(\frac{5}{4}Si^2-1)SiCos(g) \\ & -\frac{15\mu j_4 R^4}{32na^7}e(1-e^2)^{-3}(-1+8Ci^2-7Ci^4)Sin(2g) \end{aligned} \tag{2}$$

$$\begin{aligned} \dot{i}_{ob} = {} & \frac{Cot(i)}{n}\{\frac{3\mu j_3 R^3}{2a^6}e(1-e^2)^{-3}(\frac{5}{4}Si^2-1)SiCos(g) \\ & -\frac{15\mu j_4 R^4}{32a^7}e^2(1-e^2)^{-4}(-1+8Ci^2-7Ci^4)Sin(2g)\} \end{aligned} \tag{3}$$

$$\begin{aligned} \dot{h}_{ob} = {} & \frac{-Ci}{n}\{\frac{3\mu j_2 R^2}{2a^5}(1-e^2)^{-2}+\frac{\mu j_3 R^3}{8a^6}e(1-e^2)^{-3}(45Si-\frac{12}{Si})Sin(g) \\ & +\frac{3\mu j_4 R^4}{16a^7}(1+\frac{3e^2}{2})(1-e^2)^{-4}(15-35Ci^2) \\ & +\frac{15\mu j_4 R^4}{16a^7}e^2(1-e^2)(-4+7Ci^2)Cos(2g)\} \end{aligned} \tag{4}$$

$$
\begin{aligned}
g_{ob} = & \frac{-3\mu j_2 R^2}{4na^5}(1-e^2)^{-2}(1-3Ci^2) \\
& -\frac{3\mu j_3 R^3}{2na^6 e}(1+4e^2)(1-e^2)^{-3}(\frac{5}{4}Si^2-1)SiSin(g) \\
& -\frac{3\mu j_4 R^4}{64na^7}(10+\frac{15e^2}{2})(1-e^2)^{-4}(3-30Ci^2+35Ci^4) \\
& -\frac{15\mu j_4 R^4}{64na^7}(2+5e^2)(1-e^2)^{-4}(-1+8Ci^2-7Ci^4) \\
& +\frac{Cot(i)}{n}\{\frac{3\mu j_2 R^2}{2a^5}(1-e^2)^{-2}SiCi \\
& +\frac{\mu j_3 R^3}{8a^6}e(1-e^2)^{-3}(45Si^2-12)CiSin(g) \\
& +\frac{3\mu j_4 R^4}{16a^7}(1+\frac{3e^2}{2})(1-e^2)^{-4}(15-35Ci^2)CiSi \\
& +\frac{15\mu j_4 R^4}{16a^7}e^2(1-e^2)^{-4}(-4+7Ci^2)CiSiCos(2g)\}
\end{aligned}
\qquad (5)
$$

which readily give the average effects of earth oblateness including the zonal harmonics of the geopotential up to j_4.

and:

$$
\begin{aligned}
\dot{e}_{ls} = & \mu^{\frac{-1}{2}} k a^{\frac{3}{2}} \{ \sum_{M=0}^{2} \sum_{N=-1}^{1} \sum_{L=-1}^{1} e1[M,2N,2L]\sin(Mb+Ng+Lu_d) \\
& +\frac{a}{r_d}(\sum_{M=0}^{3} \sum_{N=-1}^{2} \sum_{L=-1}^{2} e2[M,2N-1,2L-1]\sin(Mb+(2N-1)g+(2L-1)u_d)
\end{aligned}
\qquad (6)
$$

$$
\begin{aligned}
\dot{i}_{ls} = & \mu^{\frac{-1}{2}} k a^{\frac{3}{2}} \{ \sum_{M=0}^{2} \sum_{N=-1}^{1} \sum_{L=-1}^{1} i1[M,2N,2L]\sin(Mb+Ng+Lu_d) \\
& +\frac{a}{r_d}(\sum_{M=0}^{3} \sum_{N=-1}^{2} \sum_{L=-1}^{2} i2[M,2N-1,2L-1]\sin(Mb+(2N-1)g+(2L-1)u_d)
\end{aligned}
\qquad (7)
$$

$$\dot{h}_{ls}=\mu^{\frac{-1}{2}}k a^{\frac{3}{2}}\{\sum_{M=0}^{2}\sum_{N=-1}^{1}\sum_{L=-1}^{1}h1[M,2N,2L]\cos(Mb+Ng+Lu_d)$$
$$+\frac{a}{r_d}(\sum_{M=0}^{3}\sum_{N=-1}^{2}\sum_{L=-1}^{2}h2[M,2N-1,2L-1]\cos(Mb+(2N-1)g+(2L-1)u_d) \quad (8)$$

$$\dot{g}_{ls}=\mu^{\frac{-1}{2}}k a^{\frac{3}{2}}\{\sum_{M=0}^{2}\sum_{N=-1}^{2}\sum_{L=-1}^{2}g1[M,2N,2L]\cos(Mb+Ng+Lu_d)$$
$$+\frac{a}{r_d}(\sum_{M=0}^{3}\sum_{N=-1}^{1}\sum_{L=-1}^{1}g2[M,2N-1,2L-1]\cos(Mb+(2N-1)g+(2L-1)u_d) \quad (9)$$

where the coefficients $e1,\ldots,g2$ *are* functions of e,i,i_d

In the subsequent development, we will classify the orbits according to the value of *a*, taking into account the relative variations of *h,g* and u_d (where the subscript *d* refers to either the moon or the sun). The ranges considered are:

$1.3R \le a < 1.4R$, $2R \le a < 3R$, $4R \le a \le 7R$.

where the ranges *1.4R-2R* , *3R-4R* are avoided due to the predominance of the radiation belts at these levels, to avoid the damages of the equipment that it may produce, beside its fatal effects on human life (for inhabited spacecrafts).

The remaining elements are considered as orbital parameters, since *a* is the element that secularly affect the relative sizes of the different perturbations.

3 Rates of the angles u_d

For the sun u_d will be denoted by u_s, while for the moon it will be denoted by u_m. As the sun completes one revolution around the earth, in the apparent geocentric orbit, in one year, u_s will have the average rate:

$$u_s=\frac{2\pi}{365.2422}rad/day$$
$$=(1.1408)10^{-5}\,\mathrm{deg/sec}.$$

Since the moon completes one revolution around the earth in one sidereal month, u_m will have the average rate:

$$\dot{u}_m = \frac{2\pi}{27.321662} rad/day$$
$$= (1.525)10^{-4} \text{ deg/sec.}$$

4 Rates of the angles *h* and *g*

We now proceed to evaluate the rates of the angles *h* and *g* for the prementioned values of *a* (in which the ranges dominated by the radiation belts are avoided) as the principal variable, with the remaining elements as parameters.

The variations of *h* and *g* come from 2 sources :

1- Variations due to the earth oblateness.

2- Variations due to the luni-solar attractions.

4.1 Oblateness variations:

(1) $\dot{h}_{ob}$:

In Eq.(4), noting that the only secular variation comes from "*a*", and substituting for the numerical values of the involved constants, we find that the order of variation of *h* due to earth oblateness, can be expressed as :

$$O(\dot{h}_{ob}) = O(\sqrt{\mu}\, j_2 R^2 a^{\frac{-7}{2}}) \; rad/sec$$
$$= O(1.593195704 \times 10^9 \times a^{-7/2}) \; deg/sec$$

(2) $\dot{g}_{ob}$:

From Eq.(5), we find that the order of variation of *g* due to the earth oblateness is the same as that of $O(\dot{h}_{ob})$.

4.2 Luni-Solar variations

(1) $\dot{h}_{ls}$:

In Eq,(8),noting that the only secular variations come from "*a*" , and substituting for the numerical values of the involved constants, we find that the order of variation of *h* due to the luni-solar attractions can be expressed as:

$$O(\dot{h}_{ls}) = O(\mu^{\frac{-1}{2}} k_m a^{\frac{3}{2}})$$

$$= O(7.8333446 x 10^{-15} a^{\frac{3}{2}}) \text{deg/sec}$$

(2) $\dot{g}_{ls}$:

From Eq.(9), we find that the order of variation of *g* due to the luni-solar attractions is the same as that of *h*.
In what follows, we tabulate the values of the orders of
Variations of *h* due to both earth oblateness and luni-solar attractions(deg/sec), which are the same as those of *g*.

$\frac{a}{R}$	$O(\dot{h}_{ob})$	$O(\dot{h}_{ls})$	$O(\dot{h})$
1	10^{-5}	10^{-9}	10^{-5}
2	10^{-6}	10^{-8}	10^{-6}
3	10^{-6}	10^{-8}	10^{-6}
4	10^{-7}	10^{-8}	10^{-7}
5	10^{-7}	10^{-8}	10^{-7}
6	10^{-7}	10^{-8}	10^{-7}
7	10^{-8}	10^{-8}	10^{-8}

Note:

It is to be noted that that the results of this table agree with Hough [12],who stated that "For semi major axes between 3 and 6 earth radii, earth oblateness and luni-solar attractions should be treated both as 1st order effects".

5 Model B

According to the order of variations of *h* and *g* (calculated in section 4) compared to those of u_d (calculated in section 3) , we find that :

$$\dot{u}_d >> \dot{h}, \dot{g} \quad for\, a > 3R$$

So , we can make further simplification by averaging over u_d to get rid of the medium periodic terms and retain only the secular and the long terms. We will call this model "Model B". Averaging over u_d, we found that :

1) The angles *g,3g* disappear.

2) The terms containing r_d disappear.

3) Only quadratic terms $<A^2,AB,AC,BC,B^2>$ u_d remain.

The complete form of model B is also of the form:

$$\dot{e}=\dot{e}_{ob}+\dot{e}_{ls}$$

$$\dot{i}=\dot{i}_{ob}+\dot{i}_{ls}$$

$$\dot{h}=\dot{h}_{ob}+\dot{h}_{ls}$$

$$\dot{g}=\dot{g}_{ob}+\dot{g}_{ls}$$

where $\dot{e}_{ob},\dot{i}_{ob},\dot{h}_{ob},\dot{g}_{ob}$ are given in Eq.s 2,3,4,5 respectively.(It is clear that these equations do not contain the angles u_d which are characteristic to the luni-solar effects).

The luni-solar terms will take the form:

$$\dot{e}_{ls}=\mu^{\frac{-1}{2}}ka^{\frac{3}{2}}\sum_{m=0}^{2}\sum_{n=-1}^{1}e[m,2n]\sin(mb+2ng) \tag{10}$$

$$\dot{i}_{ls}=\mu^{\frac{-1}{2}}ka^{\frac{3}{2}}\sum_{m=0}^{2}\sum_{n=-1}^{1}i[m,2n]\sin(mb+2ng) \tag{11}$$

$$\dot{h}_{ls}=\mu^{\frac{-1}{2}}ka^{\frac{3}{2}}\sum_{m=0}^{2}\sum_{n=-1}^{1}h[m,2n]\cos(mb+2ng) \tag{12}$$

$$\dot{g}_{ls}=\mu^{\frac{-1}{2}}ka^{\frac{3}{2}}\sum_{m=0}^{2}\sum_{n=-1}^{1}g[m,2n]\cos(mb+2ng) \tag{13}$$

The coefficients *e[m,2n],...,g[m,2n]* are given in appendix 1.

Model B is a complete model for the secular and the long periodic effects of :

1) The earth oblateness with potential up to j_4.

2) The luni-solar attractions .

This model is valid for the range $4R\le a\le 7R$, in which :

1) The radiation belts are avoided.

2) We can average over u_d only.

6 Balanced Earth Satellite Orbits

By a balanced orbit, we almost mean the two cases(or both) :

1) $\dot{h}=0$.

2) $\dot{g}=0$.

The particular importance of these elements is due to the reasons:

1) They define the coverage areas and the rates of their description (with *e*) so that their variations cause somewhat fast variations in the spatial orientation of the orbit and consequently in the coverage area of the satellite. Hence:

i) To ensure that the ground track of the satellite will scan nearly the same region on the earth surface (such that it crosses the equator in successive circuits nearly from the same point), we need to set the variation of *h* equal to zero.

ii) To ensure that the perigee and the apogee will remain fixed in space, we need to set the variation of *g* equal to zero.

2) The variations of h and g are relatively large particularly for some types of orbits.

The study of the balanced orbits is made graphically for *h* and *g* . We have two kinds of graphs to plot:

1) To plot the relation *dh/dt = 0* (*dg/dt = 0*) and get a relation between *i,a* and *e* with *h* and *g* as the parameters .

2) To plot *dh/dt* (*dg/dt*) against *i* and *a with e,h,* and *g* as the parameters.

The advantage of the 2nd group of graphs is that it gives exact values of *i* and *a* at which *h* and *g* are constants. While in the 1st group, we had to make some approximations to get the required relations but it gives us a family of balanced orbits for each graph.

The values chosen to plot at are:

e : *0,1/4,1/2*

a/R : *3,4,5,6,7*

h : *0 ,Pi/4,Pi/2*

g : *0 ,Pi/4,Pi/2*

It is found that for the curves *dh/dt=0* , the errors were very good (of order 10^{-11}-10^{-15}) except for the curves at which *g* = Pi/4 and *e* does not equal zero. So for the study of *h*, we preferred to plot curves of the 1st group (Fig.s 1.3D-10.3D), while for *g*, we plotted curves of the 2nd group (Fig.s 11.3D-38.3D). At the end of the

graphical section, we will plot curves of the 2nd group (Fig.s 39.3D-43.3D) for *dh/dt(g=Pi/4, e=1/4,1/2)*.

6.1 Orbits with fixed nodes

The families of orbits for which *dh/dt=0* (i.e with fixed nodes) are shown in the three dimensional figures (1.3D-9.3D), where the surfaces represent the values of *dh/dt* at different values of *a,i* and *e* for:

$$\{h\} \cap \{g\} = \{0, Pi/4, Pi/2\} \cap \{0, Pi/4, Pi/2\}.$$

Figure10.3D shows the effect of earth oblateness only ,where the resulting surface *dh/dt=0* is the plane *i=Pi/2*,which is clear from the equation representing *dh/dt* under the effect of the earth oblateness only.

Except for Fig.s 2,5,8.3D the equation for *dh/dt* is solved for *dh/dt=0* within an error in the range 10^{-15} -10^{-11} deg/sec (about 10^{-8} -10^{-4} deg/year)which is actually zero. For the cited figures the error increases to about 10^{-5} deg/sec which is too high. Therefor these cases (*g=Pi/4*) are treated separately by plotting *dh/dt* against *i and a* (Fig.s 38.3D-43.3D) for :

$$\{h\} \cap \{g\} \cap \{e\} = \{0, Pi/4, Pi/2\} \cap \{Pi/4\} \cap \{1/4, 1/2\}$$

The figures reveal important characteristics that are worthwhile :

1) The sensitivity to changes in *i* is small, but for *i*> 4*R* very small changes in *i* require large changes in *a* .
2) The values of *i* are very sensitive to the values of *h* but not those of *g* or *e* .

Clearly the node is fixed in regard to the perturbations produced by the earth oblateness and the luni-solar attractions, but minor changes may still be produced by the effect of the direct solar radiation pressure, and other minor perturbing influences. Also a large and unavoidable shift is produced by the eastward rotation of the earth (except for geostationary orbits) due to which, the node ,and in turn the satellite track, continuously drift westwards. But this later shift can be controlled through the choice of the semi- major axis.

6.2 Orbits with fixed perigees

The family of orbits with fixed perigees is investigated in Fig.s 11.3D-37.3D, where *dg/dt* is plotted against *i* and *a* in three dimensional representation for the *h* , *g* and *e* ranges :

$$\{h\} \cap \{g\} \cap \{e\} = \{0, Pi/4, Pi/2\} \cap \{0, Pi/4, Pi/2\} \cap \{0, 1/4, 1/2\}..$$

We note that the resulting surfaces are sensitive to changes in both *h* and *g* , but are almost not affected by *e*.

Fig.1.3D(h=0,g=0)

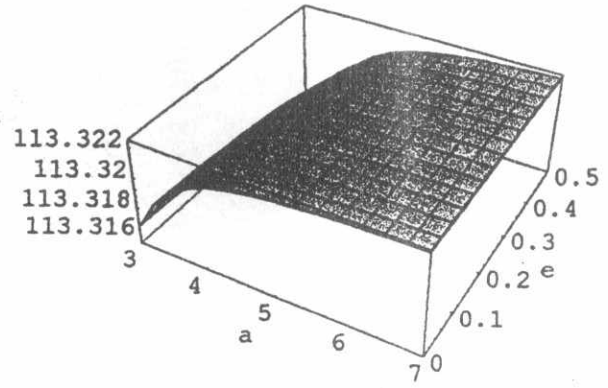

Fig.2.3D(h=0,g=Pi/4)

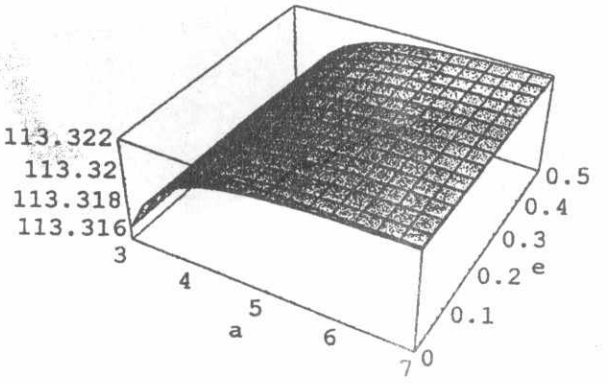

Fig.3.3D(h=0,g=Pi/2)

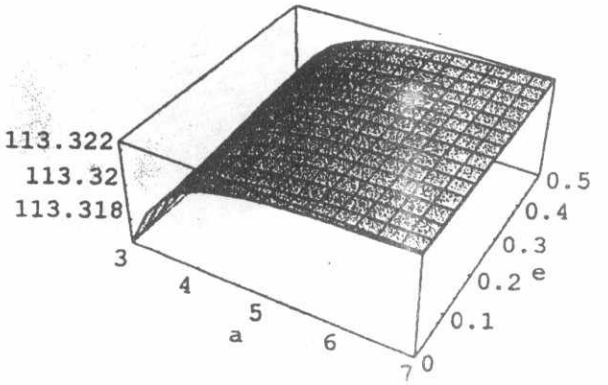

Fig.4.3D(h=Pi/4,g=0)

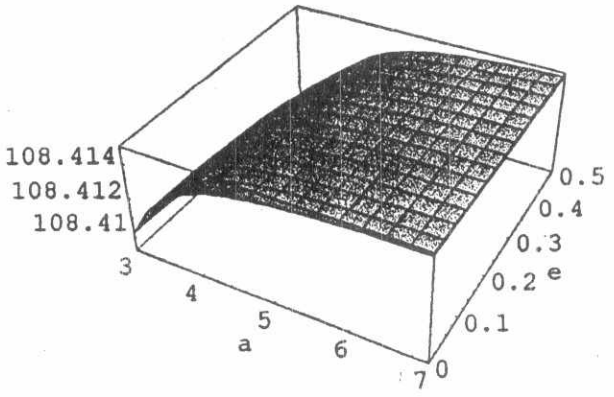

Fig.5.3D(h=Pi/4,g=Pi/4)

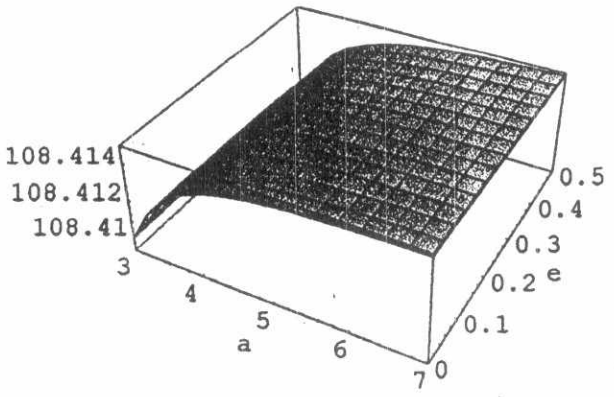

Fig.6.3D(h=Pi/4,g=Pi/2)

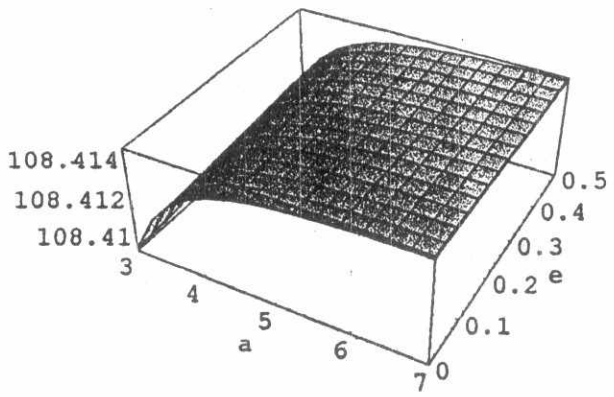

Fig.7.3D(h=Pi/2,g=0)

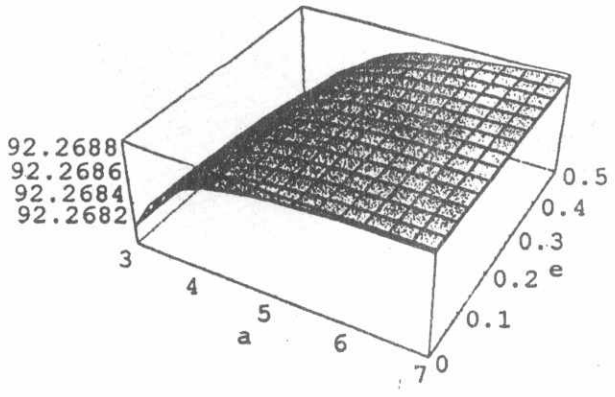

Fig.8.3D(h=Pi/2,g=Pi/4)

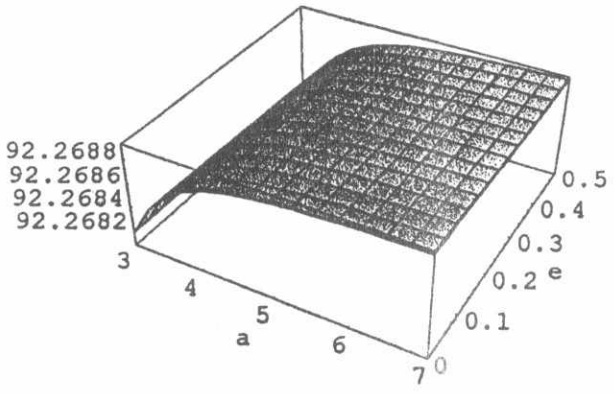

Fig.9.3D(h=Pi/2,g=Pi/2)

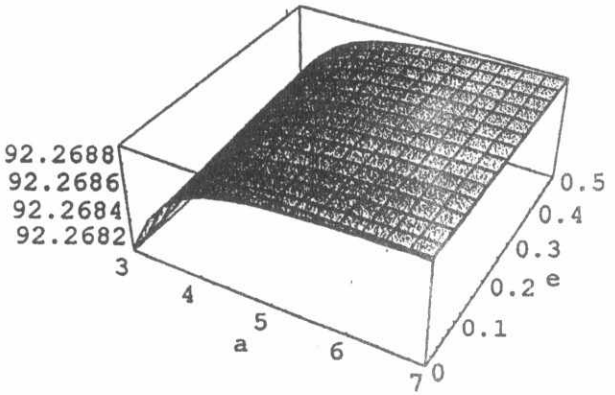

Fig.10.3D(Oblateness)

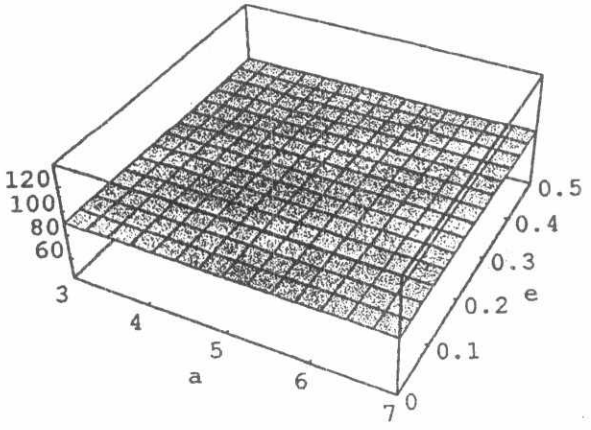

Fig.11.3D:dg/dt(h=0,g=0,e->0)

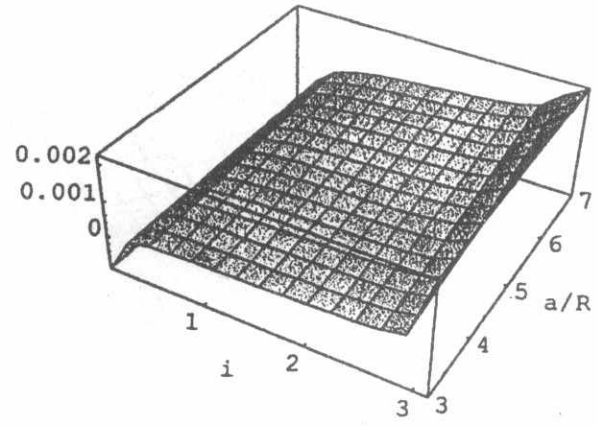

Fig.12.3D:dg/dt(h=0,g=Pi/4,e->0)

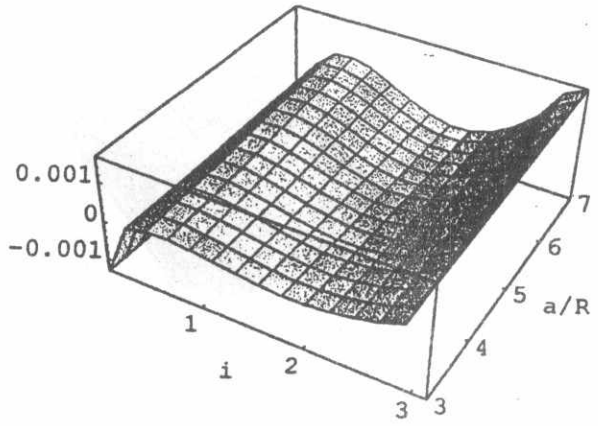

Fig.13.3D:dg/dt(h=0,g=Pi/2,e->0)

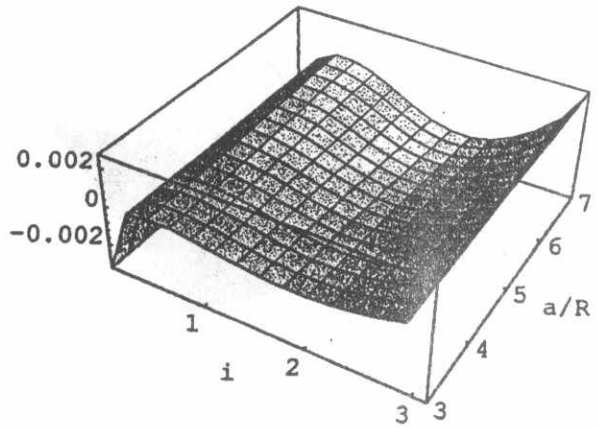

Fig.14.3D:dg/dt(h=Pi/4,g=0,e->0)

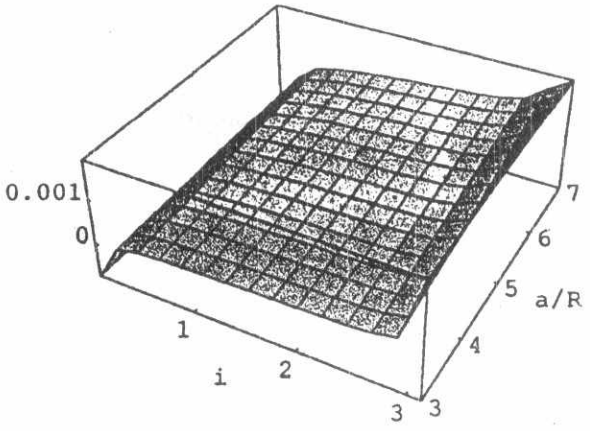

Fig.15.3D:dg/dt(h=Pi/4,g=Pi/4,e->0)

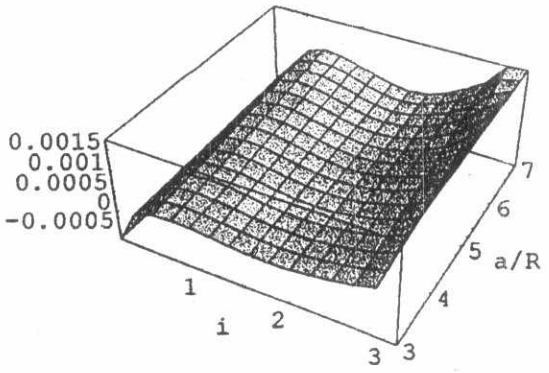

Fig.16.3D:dg/dt(h=Pi/4,g=Pi/2,e->0)

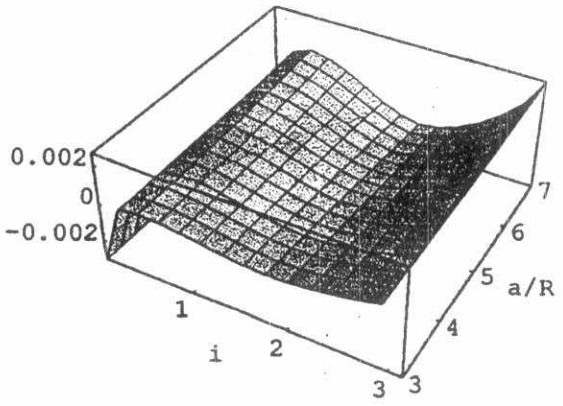

Fig.17.3D:dg/dt(h=Pi/2,g=0,e->0)

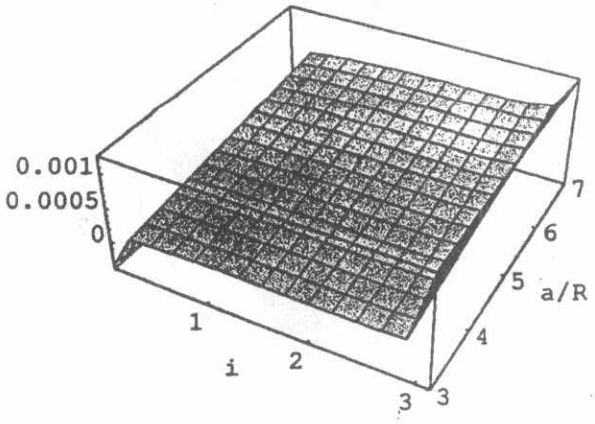

Fig.18.3D:dg/dt(h=Pi/2,g=Pi/4,e->0)

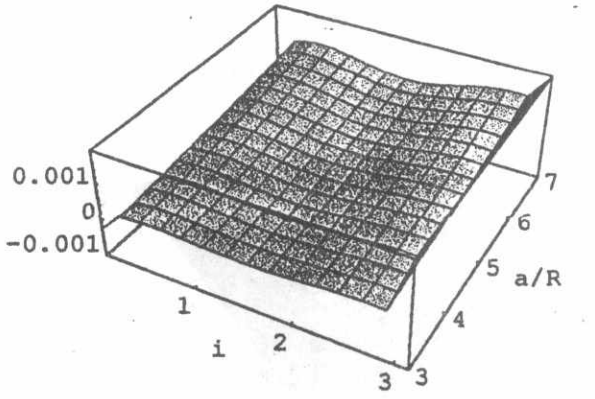

Fig.19.3D:dg/dt(h=Pi/2,g=Pi/2,e->0)

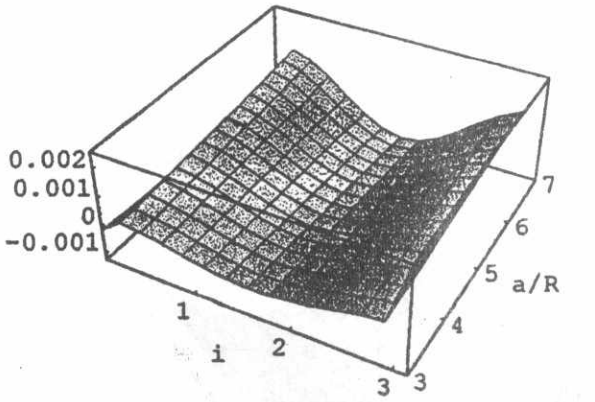

Fig.20.3D:dg/dt(h=0,g=0,e=1/4)

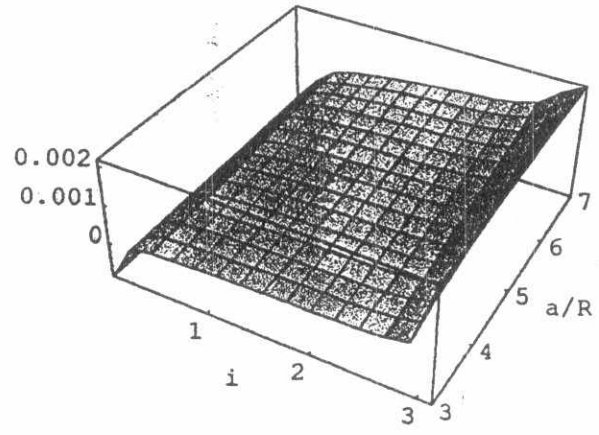

Fig.21.3D:dg/dt(h=0,g=Pi/4,e=1/4)

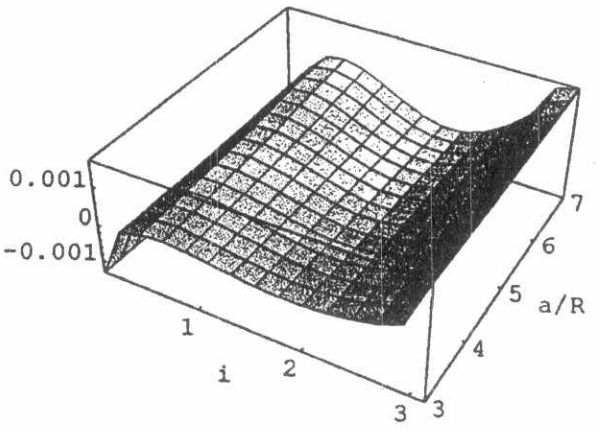

Fig.22.3D:dg/dt(h=0,g=Pi/2,e=1/4)

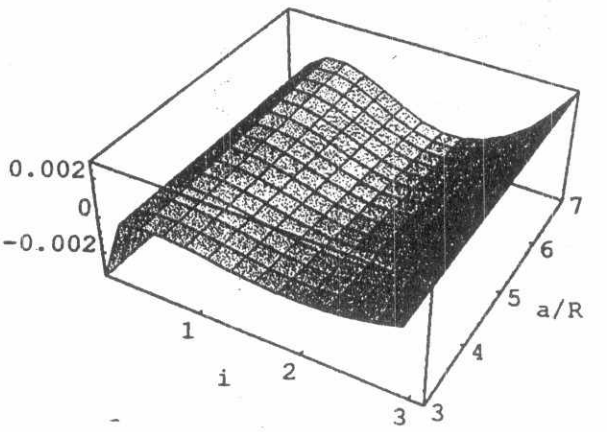

Fig.23.3D:dg/dt(h=Pi/4,g=0,e=1/4)

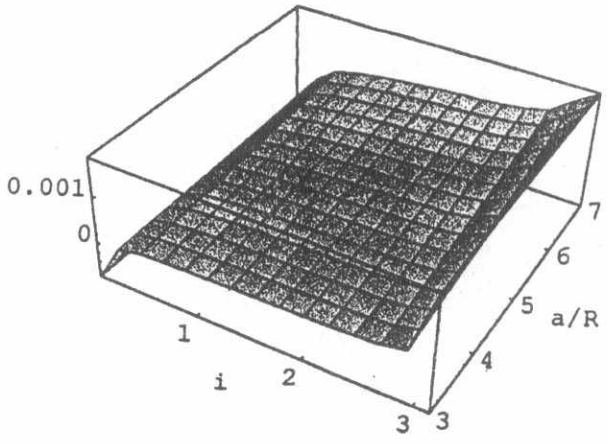

Fig.24.3D:dg/dt(h=Pi/4,g=Pi/4,e=1/4)

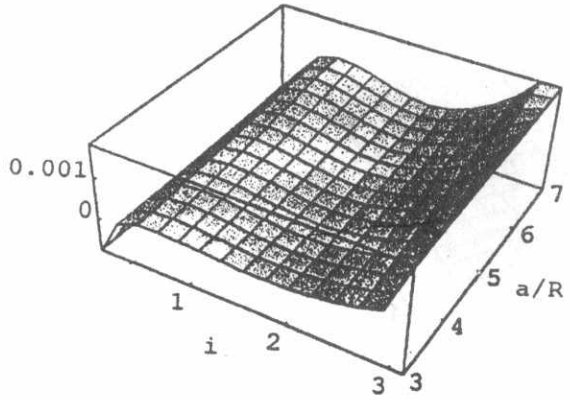

Fig.25.3D:dg/dt(h=Pi/4,g=Pi/2,e=1/4)

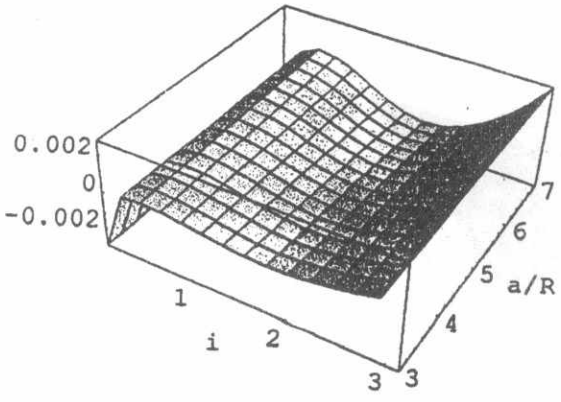

Fig.26.3D:dg/dt(h=Pi/2,g=0,e=1/4)

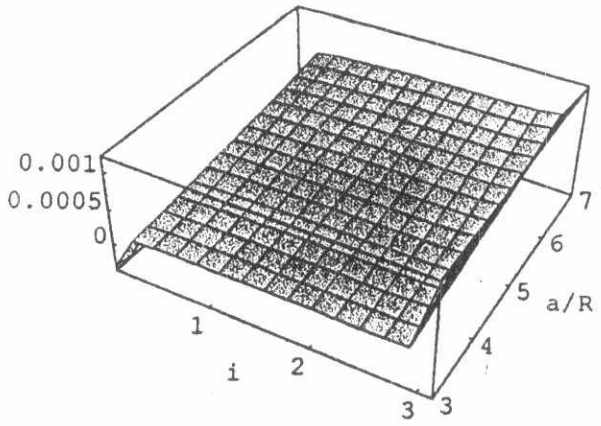

Fig.27.3D:dg/dt(h=Pi/2,g=Pi/4,e=1/4)

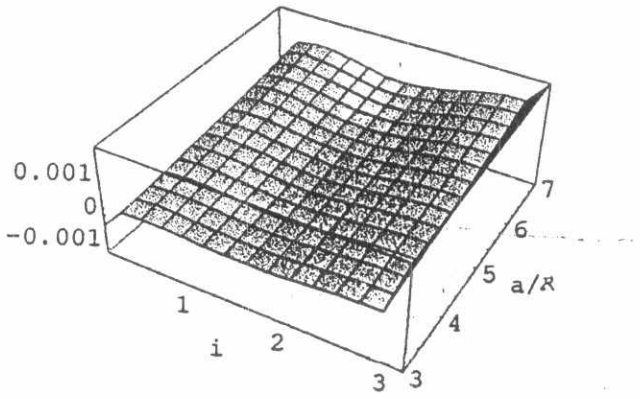

Fig.28.3D:dg/dt(h=Pi/2,g=Pi/2,e=1/4)

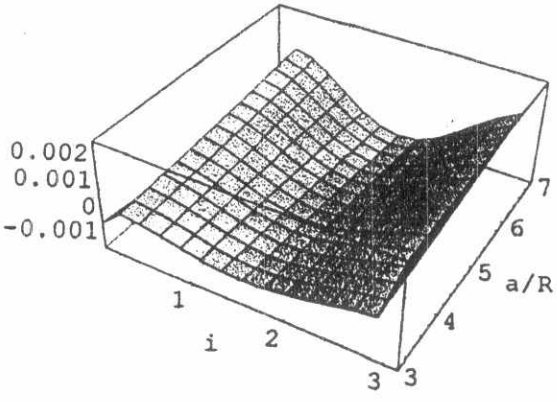

Fig.29.3D:dg/dt(h=0,g=0,e=1/2)

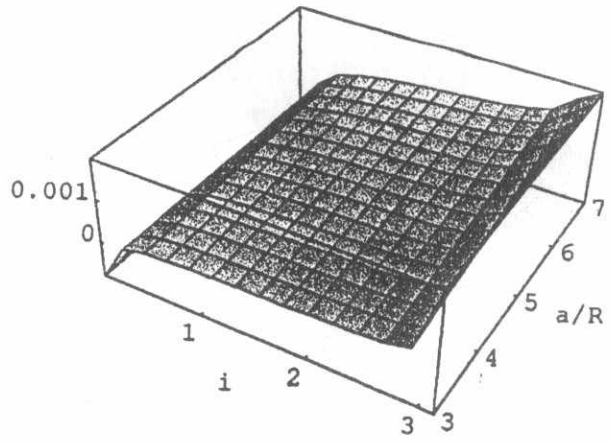

Fig.30.3D:dg/dt(h=0,g=Pi/4,e=1/2)

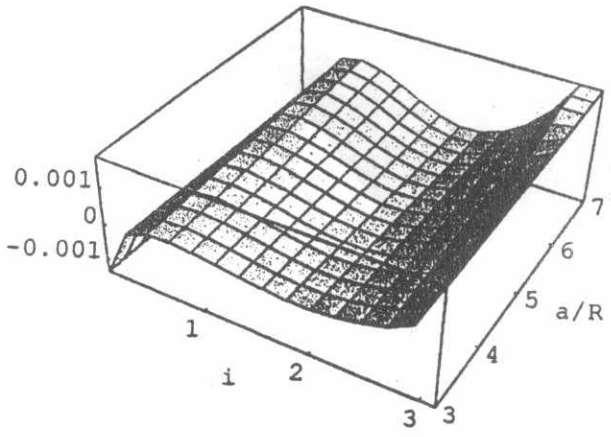

Fig.31.3D:dg/dt(h=0,g=Pi/2,e=1/2)

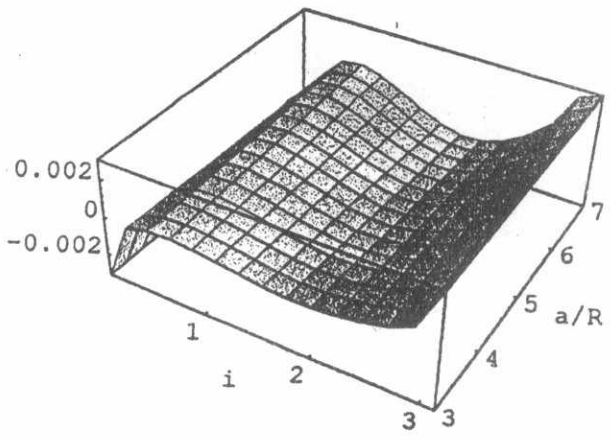

Fig.32.3D:dg/dt(h=Pi/4,g=0,e=1/2)

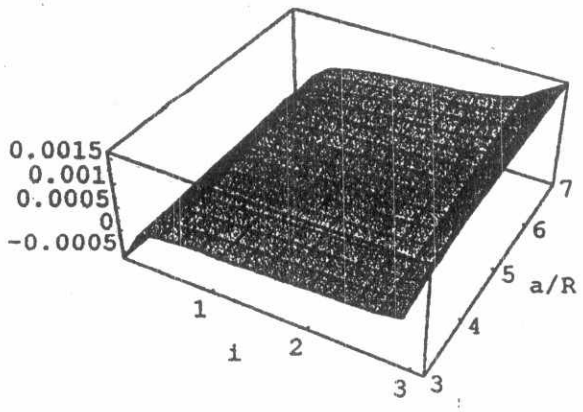

Fig.33.3D:dg/dt(h=Pi/4,g=Pi/4,e=1/2)

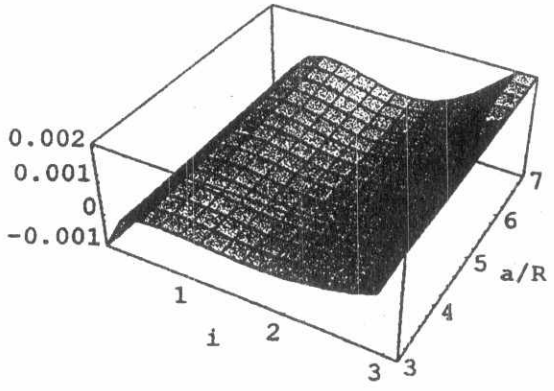

Fig.34.3D:dg/dt(h=Pi/4,g=Pi/2,e=1/2)

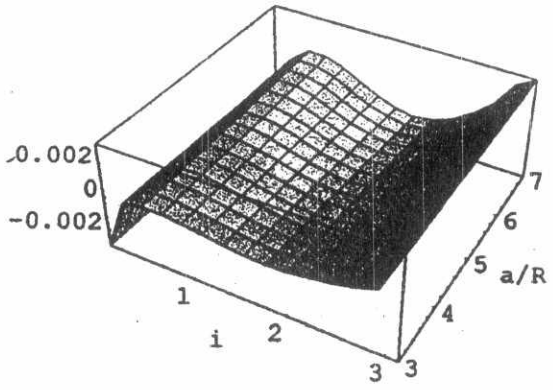

Fig.35.3D:dg/dt(h=Pi/2,g=0,e=1/2)

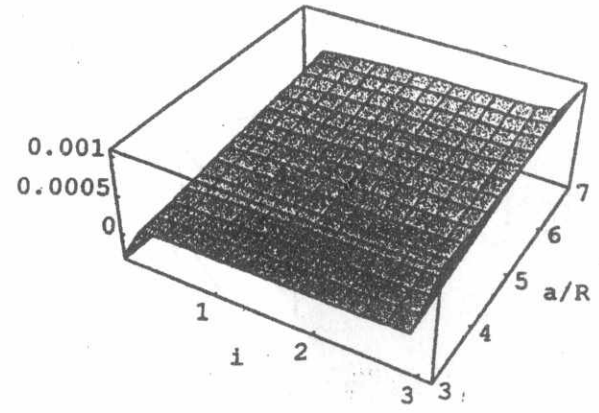

Fig.36.3D:dg/dt(h=Pi/2,g=Pi/4,e=1/2)

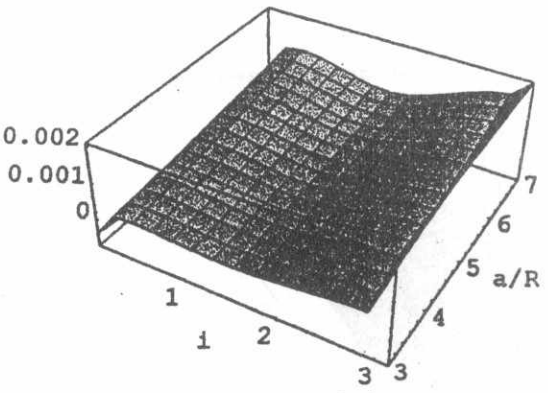

Fig.37.3D:dg/dt(h=Pi/2,g=Pi/2,e=1/2)

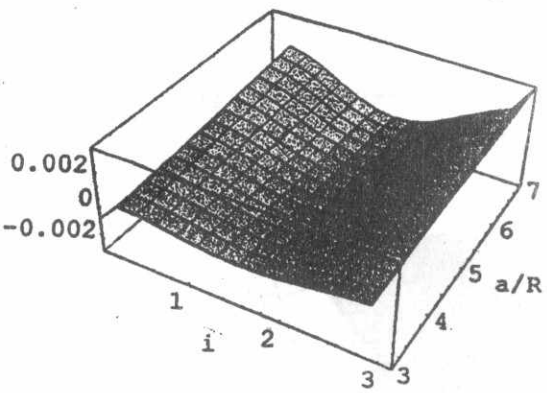

Fig.38.3D:dh/dt(h=0,g=Pi/4,e=1/4)

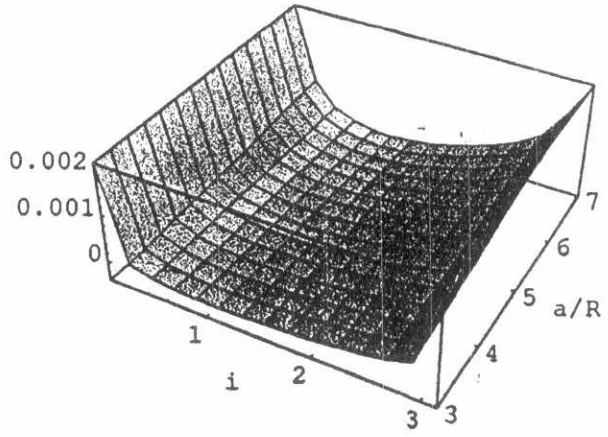

Fig.39.3D:dh/dt(h=Pi/4,g=Pi/4,e=1/4)

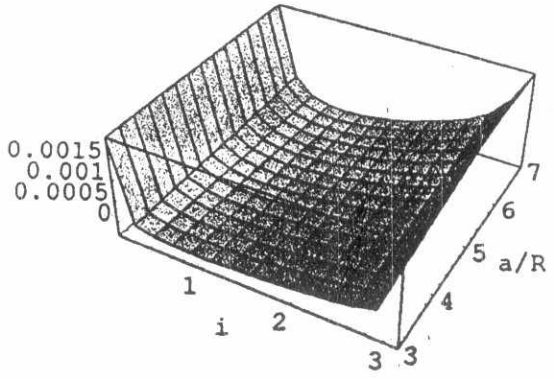

Fig.40.3D:dh/dt(h=Pi/2,g=Pi/4,e=1/4)

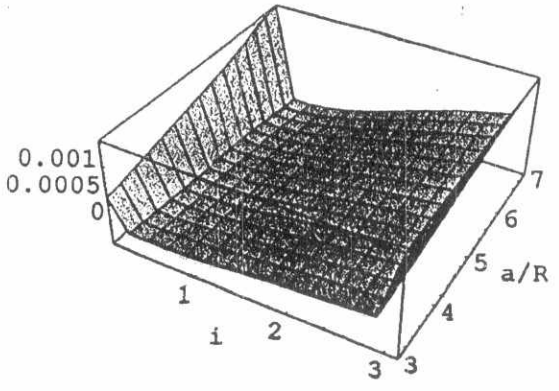

Fig.41.3D:dh/dt(h=0,g=Pi/4,e=1/2)

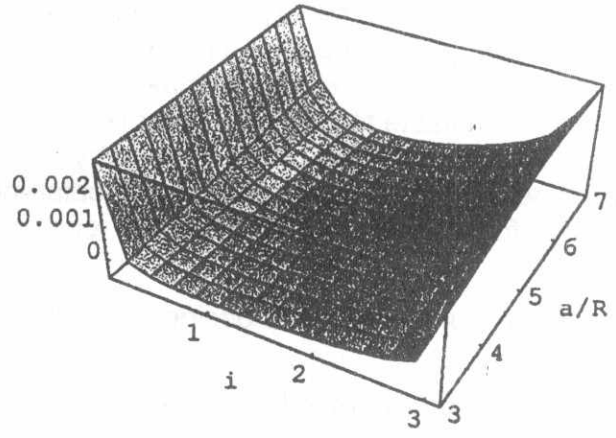

Fig.42.3D:dh/dt(h=Pi/4,g=Pi/4,e=1/2)

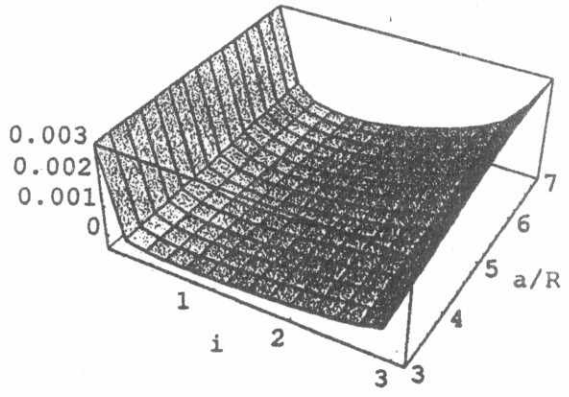

Fig.43.3D:dh/dt(h=Pi/2,g=Pi/4,e=1/2)

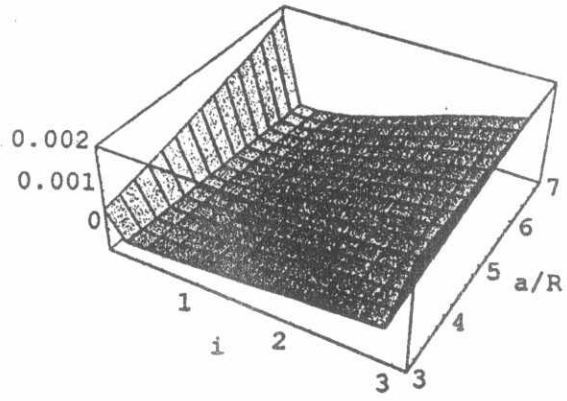

6.3 Balanced Orbits

Let balanced orbits be defined as those for which both the node and the perigee remain fixed under the combined perturbation effects due to both the earth oblateness and the luni-solar attraction. The above analysis then shows that such an orbit will be balanced within a reliable tolerance only for few weeks since we are forced to accept the motion of either the node or the perigee by about 10^{-5} deg/sec. The reason is that the major perturbing influence is the earth oblateness, and under this effect $dh/dt=0$ (exactly) for $i \sim Pi/2$, while $dg/dt=0$ only near the critical inclination

i_c = 63.4 deg. Hence the best procedure is to design a satellite constellation for which :

1) The nodal shifts due to the perturbative effects and earth rotation are modeled to yield continuous coverage .
2) The perigees are either fixed or arranged to realize that the perigee (or the apogee) be overhead the coverage region (regions) in due times. This may require near commmensurability with the admitted nodal periods.

References

[1] Kudielka, V., "Balanced Earth Satellite Orbits" Celest. Mech. 60 (1994).
[2] Coffey,et al., "Frozen Orbits for Satellites Close to an Earth-Like Planet" Celest. Mech. 59 (1994).
[3] Lara, et al., "Numerical Continuation of Families of Frozen Orbits in The Zonal Problem of Artificial Satellite Theory" Celest. Mech. 62 (1995).
[4] Brouwer "Solution of the Problem of Artificial Satellite Theory Without Drag" Astron. J. 64 (1959)
[5] Kozai ,Y "Second-Order Solution Of Artificial Satellite Theory Without Air Drag " Astron. J. 67 (1962).
[6] Kozai ,Y "The Motion of A close Earth Satellite " Astron. J. 64 (1959).
[7] Musen ,P "The influence of Solar Radiation Pressure on the Motion of an Artificial Satellite" J. Geoph. Res. 65 No.5 (1960) .
[8] Cook ,G .E "Lunar-Solar Perturbations of the Orbit of an Earth Satellite " Roy. Astron. Soc. Vol. 6 , No.3 (1962).
[9] Lane , M.T. "an Analytic Modeling of Lunar Perturbations of Artificial Satellites of the Earth " Celest. Mech. 46 , 287 (1989) .
[10] Delhaise ,F ; and Morbidelli , A "Luni-Solar Effects of Geosynchronous Orbits at the Critical Inclination " Celest. Mech. 57 , 155 (1993).
[11] S.M.Elshabouri ,et.al., " Averaged Effects of Earth Oblateness and Luni-Solar Attractions",Submitted for pub. In the Bult. Fac. Sci. Cairo Univ.(1999)
[12] Hough,M,E ,"Orbits Near Critical Inclination, Including Luni-Solar Perturbations ",Celst. Mech. 25 (1981).

Appendix 1
The coefficients of Model B

$$e[0,-2]=0$$

$$e[0,0]=0$$

$$e[0,2]=(15\,e\,\mathrm{Sqrt}[1-e^2]\,(1-Ci^2+Cid^2-Ci^2\,Cid^2-2\,Si\,Sid))/16$$

$$e[1,-2]=\frac{15\,(-1+Ci)\,Cid\,e\,\mathrm{Sqrt}[1-e^2]\,Si\,Sid}{8}$$

$$e[1,0]=0$$

$$e[1,2]=\frac{-15\,(1+Ci)\,Cid\,e\,\mathrm{Sqrt}[1-e^2]\,Si\,Sid}{8}$$

$$e[2,-2]=\frac{-15\,(-1+Ci)^2\,e\,\mathrm{Sqrt}[1-e^2]\,Sid^2}{32}$$

$$e[2,0]=0$$

$$e[2,2]=\frac{15\,(1+Ci)^2\,e\,\mathrm{Sqrt}[1-e^2]\,Sid^2}{32}$$

$$i[0, -2] = 0$$

$$i[0, 0] = 0$$

$$i[0, 2] = \frac{15\, Ci\, e^2\, Si\, (-2\, Cid^2 + Sid^2)}{16\, Sqrt[1 - e^2]^2}$$

$$i[1, -2] = \frac{15\, Cid\, e^2\, (-Ci^2 + Si + Si^2)\, Sid}{16\, Sqrt[1 - e^2]^2}$$

$$i[1, 0] = \frac{3\, Cid\, (2 + 3\, e^2)\, Si\, Sid}{8\, Sqrt[1 - e^2]^2}$$

$$i[1, 2] = \frac{15\, Cid\, e^2\, (Ci^2 + Si - Si^2)\, Sid}{16\, Sqrt[1 - e^2]^2}$$

$$i[2, -2] = \frac{-15\, Ci\, e^2\, (1 + Si)\, Sid^2}{32\, Sqrt[1 - e^2]^2}$$

$$i[2, 0] = \frac{-3\, Ci\, (2 + 3\, e^2)\, Sid^2}{16\, Sqrt[1 - e^2]^2}$$

$$i[2, 2] = \frac{15\, Ci\, e^2\, (-1 + Si)\, Sid^2}{32\, Sqrt[1 - e^2]^2}$$

$$h[0,-2]=\frac{15\,Ci\,e^{2}\,Si\,(2\,Cid^{2}-Sid^{2})}{16\,Sqrt[1-e^{2}]}$$

$$h[0,0]=0$$

$$h[0,2]=\frac{15\,Ci\,e^{2}\,Si\,(2\,Cid^{2}-Sid^{2})}{16\,Sqrt[1-e^{2}]}$$

$$h[1,-2]=\frac{15\,Cid\,e^{2}\,(-Ci^{2}+Si+Si^{2})\,Sid}{16\,Sqrt[1-e^{2}]}$$

$$h[1,0]=\frac{3\,Cid\,(2+3\,e^{2})\,(Ci^{2}-Si^{2})\,Sid}{8\,Sqrt[1-e^{2}]}$$

$$h[1,2]=\frac{15\,Cid\,e^{2}\,(-Ci^{2}-Si+Si^{2})\,Sid}{16\,Sqrt[1-e^{2}]}$$

$$h[2,-2]=\frac{-15\,Ci\,e^{2}\,(1+Si)\,Sid^{2}}{32\,Sqrt[1-e^{2}]}$$

$$h[2,0]=\frac{3\,Ci\,(2+3\,e^{2})\,Si\,Sid^{2}}{16\,Sqrt[1-e^{2}]}$$

$$h[2,2]=\frac{15\,Ci\,e^{2}\,(1-Si)\,Sid^{2}}{32\,Sqrt[1-e^{2}]}$$

$$g[0,-2]=\frac{15\,Ci\,e^2\,Si\,(2\,Cid^2-Sid^2)}{16\,Sqrt[1-e^2]}$$

$$g[0,0]=0$$

$$g[0,2]=\frac{15\,Ci\,e^2\,Si\,(2\,Cid^2-Sid^2)}{16\,Sqrt[1-e^2]}$$

$$g[1,-2]=\frac{15\,Cid\,e^2\,(-Ci^2+Si+Si^2)\,Sid}{16\,Sqrt[1-e^2]}$$

$$g[1,0]=\frac{3\,Cid\,(2+3\,e^2)\,(Ci^2-Si^2)\,Sid}{8\,Sqrt[1-e^2]}$$

$$g[1,2]=\frac{15\,Cid\,e^2\,(-Ci^2-Si+Si^2)\,Sid}{16\,Sqrt[1-e^2]}$$

$$g[2,-2]=\frac{-15\,Ci\,e^2\,(1+Si)\,Sid^2}{32\,Sqrt[1-e^2]}$$

$$g[2,0]=\frac{3\,Ci\,(2+3\,e^2)\,Si\,Sid^2}{16\,Sqrt[1-e^2]}$$

$$g[2,2]=\frac{15\,Ci\,e^2\,(1-Si)\,Sid^2}{32\,Sqrt[1-e^2]}$$